A Letters Journal Exploring the Frontiers of Physics

August 2009

EPL, **87** (2009) 48011
doi: 10.1209/0295-5075/87/48011

www.epljournal.org

Swarming dynamics in bacterial colonies

H. P. Zhang[(a)], Avraham Be'er, Rachel S. Smith, E.-L. Florin and Harry L. Swinney

Center for Nonlinear Dynamics and Department of Physics, The University of Texas at Austin Austin, TX 78712, USA

received 17 July 2009; accepted in final form 14 August 2009
published online 15 September 2009

PACS 87.18.Gh – Cell-cell communication; collective behavior of motile cells
PACS 47.63.Gd – Swimming microorganisms
PACS 05.65.+b – Self-organized systems

Abstract – We determine and relate the characteristic velocity, length, and time scales for bacterial motion in swarming colonies of *Paenibacillus dendritiformis* growing on semi-solid agar substrates. The bacteria swim within a thin fluid layer, and they form long-lived jets and vortices. These coherent structures lead to anisotropy in velocity spatial correlations and to a two-step relaxation in velocity temporal correlations. The mean squared displacement of passive tracers exhibits a short-time regime with nearly ballistic transport and a diffusive long-time regime. We find that various definitions of the correlation length all lead to length scales that are, surprisingly, essentially independent of the mean bacterial speed, while the correlation time is linearly proportional to the ratio of the correlation length to the mean speed.

Collections of self-propelled objects, such as vibrating rods [1,2], flocking birds [3], and fish schools [4], often exhibit collective dynamics with extended spatiotemporal coherence. This biologically originated phenomenon has been studied from perspectives of nonequilibrium statistical mechanics and nonlinear dynamics. The studies have used discrete-particle dynamics based on simple local-interaction laws [5,6], continuum ideas from liquid-crystal physics [7], two-fluid models [8,9], and hydrodynamics [10], and have simulated numerically idealized swimmers [11–13].

Coherent motions have been observed in suspensions of swimming bacteria. Dombrowski *et al.* [14] observed vortices and jets with a length scale $\sim 20\,\mu$m and a correlation time of 1–2 s in suspensions of *Bacillus subtilis,* where bioconvection was driven by chemotaxis and a Rayleigh-Taylor instability. Wu and Libchaber [15] tracked particles suspended in a soap film containing motile *Escherichia coli* and found that the mean squared displacement $\langle \Delta r^2(\Delta t) \rangle$ of the passive tracers exhibited a short-time regime with nearly ballistic transport and a long-time regime with diffusive transport; they conjectured that the transition time from short to long time scales was set by the lifetime of the coherent structures. Sokolov *et al.* [16] studied swarming of *B. subtilis* in a soap film and found that the correlation lengths varied smoothly and monotonically as the bacterial concentration increased.

Collective dynamics has also been observed in bacterial colonies (*e.g., B. subtilis* and *E. coli* [17–22]), grown on an agar gel substrate. On the surface of a gel, swimming bacteria from a suspension differentiate into "swarmers", which are generally larger in size and have more flagella than the bacteria in suspension. Swarmers extract from an agar substrate nutrients and water, which mix with extracellular materials secreted by bacteria, such as polysaccharide, and form a thin slime layer. In this layer, densely packed swarmers move rapidly in coordinated motion.

Although some experimental studies have been made to characterize the dynamics of swarming bacteria on an agar substrate [20–22], the relationship between the length, time, and velocity scales of the motion has not been systematically explored. We address this problem in a study of colonies of *Paenibacillus dendritiformis* bacteria. We determine the speeds of individual bacteria and the velocity field within colonies of the bacteria, and we obtain the relation between the bacterial mean speed and the correlation length and correlation time for the coherent swarming motion.

Experiment. – Colonies of *P. dendritiformis* (Morphotype *T*) [23,24] are grown on substrates made of 1 liter solution of deionized water in which is dissolved 4 g of Bacto Peptone, 5 g of K_2HPO_4, 5 g of NaCl, and Difco Bacto agar. The agar mass varies from 10 g to 16 g, yielding agar concentrations 1.0–1.6%. We pour 12 ml of the solution into an 8.8 cm diameter Petri dish and

[(a)]E-mail: zhang@chaos.utexas.edu

maintain the dish for 4 days at 25 °C and 50% humidity before inoculation.

The bacteria are stored at −80 °C in Luria Broth (LB) (Sigma) with 25% glycerol. LB was inoculated with the frozen stock and grown for 24 hours at 30 °C with shaking; it reached an OD_{650} (optical density) of 1.0, corresponding to approximately 1×10^8 bacteria/ml, measured by counting colonies inoculated on LB plates after culture dilution.

The agar substrates are inoculated by placing 5 μl of the culture on the surface, forming a 5 mm diameter circular colony. The inoculated gel is stored in an incubator at 30 °C and 90% humidity. After a lag time of 18 h, a colony starts to expand outward and develops an intricate branched pattern within a well-defined circular envelope. The speed of the growing envelope, typically 0.05 μm/s, depends on the agar concentration [22]. Collective motion occurs at the growing edge of the colony, where the rod-like (4 μm × 0.8 μm) bacteria swim in a fluid layer about a few μm thick. The density of closely packed bacteria at the colony's edge is estimated to be 2×10^{11} bacteria/ml.

Bacterial motion is imaged using an optical microscope (Olympus IX50) equipped with an LD 60X Phase contrast (PH2) objective lens. A CCD camera captures the bacterial motion at a rate of 30 frames/s with a spatial resolution of 1004 × 997 pixels over a field of view of $120 \times 120\,\mu m^2$. Images are directly streamed to a hard disk for 600 s periods, corresponding to 18000 images. The time series is sufficiently long compared to the velocity correlation time (typically 4 s) so that statistically significant values can be obtained for the velocity correlation length and time scales, and different regimes of transport can be distinguished. Individual bacteria are resolved in the images and serve as tracers for particle image velocimetry (PIV) analysis, which is used to obtain 2-dimensional velocity fields. The velocities from PIV are interpolated using cubic splines to obtain a regular 100 × 100 grid with a spatial resolution of 1.2 μm with 5% RMS errors.

The motion of particles in the flow field is deduced by releasing passive numerical tracers in the velocity field determined from PIV analysis. As an independent check of the statistics obtained from these numerical tracers, we made physical measurements, releasing 2 μm diameter silica beads in the bacterial colonies. The beads are small enough in size and number (∼one per 500 μm^2) so that they serve as passive tracers. Trajectories of the physical tracers are extracted from sequential images using a particle tracking algorithm.

Results. – The instantaneous velocity field images reveal intense jets, some of which are ten times as long as the 4 μm bacteria; see those centered at (44 μm, 34 μm) and (45 μm, 12 μm) in fig. 1. Coherent vortices, typically 10 μm in diameter, are also readily evident; see those centered at (10 μm, 9 μm) and (31 μm, 46 μm).

The mean speed $\overline{V}$ exhibits a strong dependence on agar concentration, decreasing by a factor of three over the concentration range studied; see the inset of fig. 1. This observation is consistent with previous studies that have shown that the underlying substrate with suitable agar concentration is one of the most critical requirements for swarming [17–19,25]. An increase in agar concentration leads to less water being extracted from the gel and hence a thinner lubricating layer. Further, the bacteria in the thinner layer could produce about the same amount of extracellular material, so a thinner layer would also have

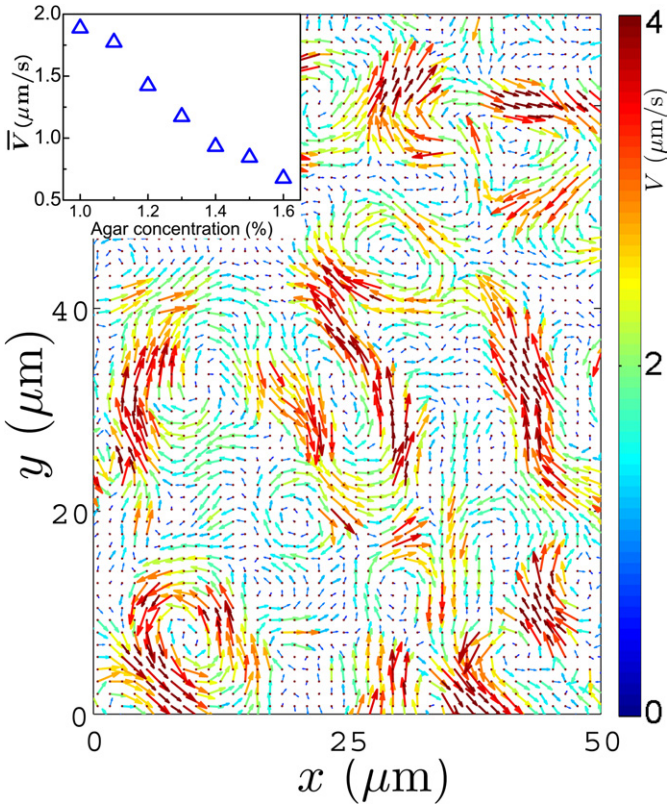

Fig. 1: (Color online) Instantaneous velocity field for bacteria near the edge of a growing colony (for agar concentration 1.3%). Both the length and color (see color bar) of the arrows represent the magnitude of the velocity; for clarity, only 35% of the velocity vectors are plotted. The speed averaged in both space and time is plotted as a function of agar concentration in the inset. Movies of the flow field (`BacteriaFlow.avi` and `VelField.avi`[1]) and a picture of the growing colony (`WholeColony.jpg`[2]) are in the on-line supplementary material[3].

[1]The movie `BacteriaFlow.avi` is compiled from phase-contrast images of moving bacteria in a colony with 1.3% agar concentration. The image window is 115 μm × 115 μm. The movie is played in real time. The movie `VelField.avi` shows instantaneous velocity fields of bacteria. A typical stationary picture is shown in fig. 1. Data were obtained in a colony with 1.3% agar concentration. The image window is 115 μm × 115 μm. The movie is played in real time.

[2]The picture `WholeColony.jpg` shows the *P. dendritiformis* bacterial colony grown on a 1.3% (wt/vol) agar gel with 4 g/liter peptone. Microscopic velocity measurements were carried out at the growing edge, as indicated by the red arrow. The petri-dish is 88 mm in diameter, while the image window in fig. 1 is 50 μm × 70 μm.

[3]High-resolution versions of the movies are available at: `chaos.utexas.edu/~zhang/BacFlow/Bac.htm`.

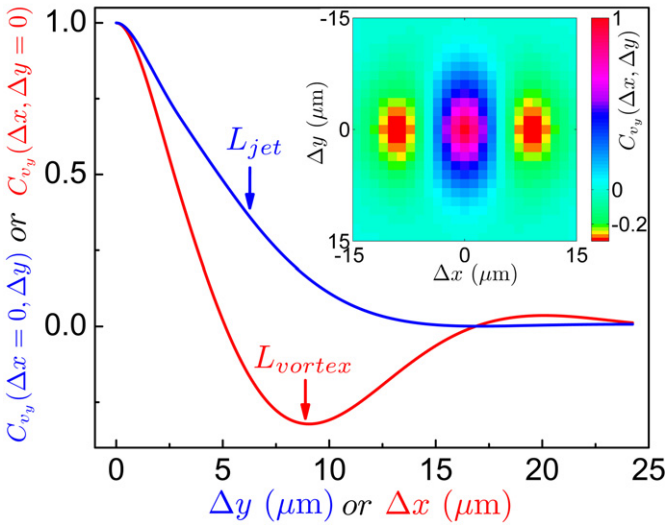

Fig. 2: (Color online) Spatial correlation function of the y-component of the instantaneous velocity v_y is shown in the inset (measured in a colony with 1.3% agar concentration). A profile of the correlation function $C_{v_y}(\Delta x, \Delta y = 0)$ along the x-axis is given by the red curve in the graph; the minimum correlation is negative (anti-correlation), yielding the characteristic size of the vortices, 9.1 μm (see arrow). A profile of the correlation function $C_{v_y}(\Delta x = 0, \Delta y)$ along the y-axis is given by the blue curve in the graph; the $1/e$ value yields the characteristic size of the jets, 6.2 μm (see arrow).

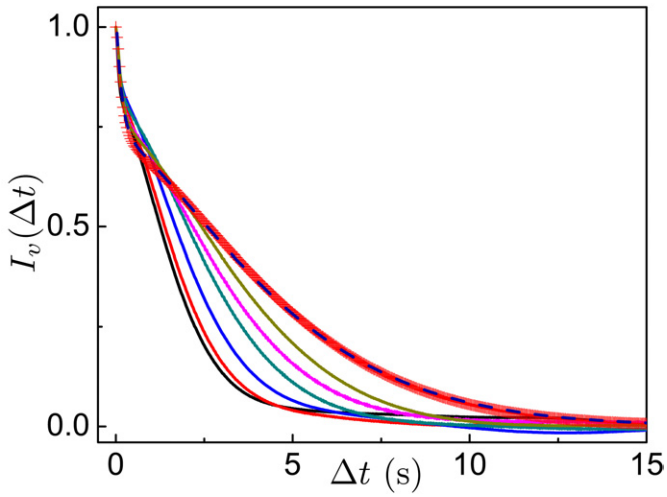

Fig. 3: (Color online) Temporal correlation functions of velocity fields measured for seven different agar concentrations (from left to right: 1.0% to 1.6% in steps of 0.1%) exhibit a two-step relaxation. The fast process is exponential and depends weakly on the agar concentration. The slow relaxation depends on the agar concentration and can be described by a stretched-exponential function. The result from the case of 1.6% is shown by red crosses (top curve at $\Delta t = 5$ s) and the dashed line is a fit to eq. (3) (see text).

higher concentration of extracellular material, therefore higher viscosity, which would decrease the speeds, in accord with the inset of fig. 1. This interpretation is supported by the following experimental observations. In experiments, where we use silica beads as passive tracers, we observe that beads move out of the focal plane much less frequently in colonies on substrates with high agar concentrations, which suggests a thinner slime layer with better confinement.

To quantify the spatial correlation demonstrated by vortices and jets in fig. 1, we compute the 2-dimensional spatial correlation function of instantaneous velocity components, which for the y-component is defined as

$$C_{v_y}(\Delta x, \Delta y) = \frac{\langle v_y(x,y,t) v_y(x+\Delta x, y+\Delta y, t)\rangle}{\langle v_y(x,y,t) v_y(x,y,t)\rangle}, \quad (1)$$

where $\langle \ldots \rangle$ represents average over time t and space (x, y). The correlation function is anisotropic, as shown in the inset of fig. 2. Profiles along the x-axis (the transverse correlation function, $\Delta y = 0$), and along the y-axis (the longitudinal correlation function, $\Delta x = 0$) are shown in the main panel by red and blue lines, respectively (fig. 2). The longitudinal correlation function $C_{v_y}(\Delta x = 0, \Delta y)$ decays exponentially from the origin to zero value, and no negative correlation is seen. We identify the jet length L_{jet} as the $1/e$ decay length in the longitudinal correlation function. However, many jets have a length that is as much as 5–8 times larger than L_{jet}; for example, see the jet at (44 μm, 34 μm) in fig. 1. The transverse correlation function develops a strong negative correlation with a minimum corresponding to the characteristic length scale for the vortices: L_{vortex}. Similar negative velocity correlation has been reported in recent numerical studies based on idealized swimmers [26].

We compute velocity temporal correlation function to quantify the lifetime of the coherent structures:

$$I_v(\Delta t) = \frac{\langle \vec{v}(x,y,t) \cdot \vec{v}(x,y,t+\Delta t)\rangle}{\langle \vec{v}(x,y,t) \cdot \vec{v}(x,y,t)\rangle}. \quad (2)$$

$I_v(\Delta t)$ computed for seven agar concentrations is shown in fig. 3. All temporal correlation functions exhibit a two-step relaxation. The fast relaxation occurs within 0.1 seconds, which is barely resolved in our data. The second slower relaxation represents processes of coherent structure disintegration, which we found can be best described by a stretched exponential function, instead of a simple exponential decay. Therefore, the whole temporal correlation function can be fitted to

$$I_v(\Delta t) = A \exp^{-\Delta t/T_1} + B \exp^{-(\Delta t/T_{cor})^{\beta}}, \quad (3)$$

where a stretching parameter $\beta = 1.4$ is found to fit data at all agar concentrations. We note that a two-step relaxation process described by eq. (3) has been widely observed in physical systems exhibiting glassy dynamics [27], but in those systems the stretching parameter β is usually less than unity.

The vortices and jets also affect the motion of tracer particles. For example, the mean square displacement of tracer particles, $\langle \Delta r^2(\Delta t)\rangle = \langle (\vec{r}(t+\Delta t) - \vec{r}(t))^2\rangle$, is

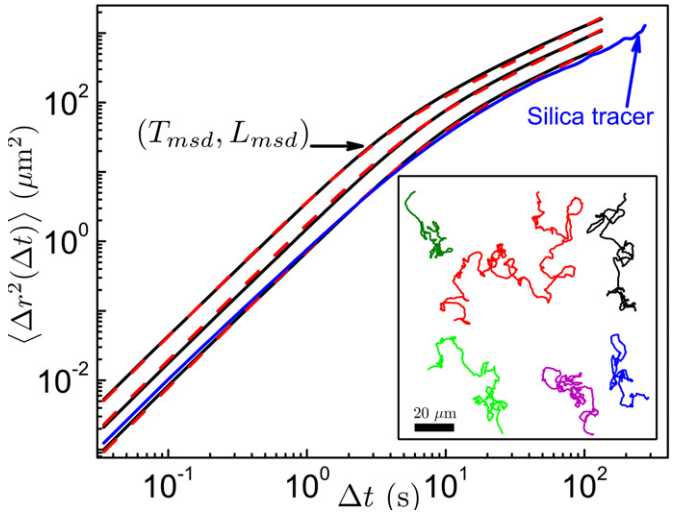

Fig. 4: (Color online) Mean square displacement $\langle \Delta r^2(\Delta t)\rangle$ as a function of time separation Δt for imaginary passive tracers advected by the measured velocity field (black solid lines) and for real silica bead tracers (blue lines). Agar concentrations are 1.0%, 1.3% and 1.5% from left to right. $\langle \Delta r^2(\Delta t)\rangle$ exhibits two distinct regimes, a short-time regime with nearly ballistic transport, and a longer-time regime with diffusive transport. The length and time that correspond to the transition from ballistic to diffusive regime, T_{msd} and L_{msd}, are indicated by an arrow. The dashed lines are fits of eq. (4). The inset shows six typical trajectories, each for a 300 s time interval. Movies of numerical (`NumericalTracer.avi`[4]) and physical (`SilicaBeads.avi`[5]) tracers can be found in supplementary materials (see footnote [3]).

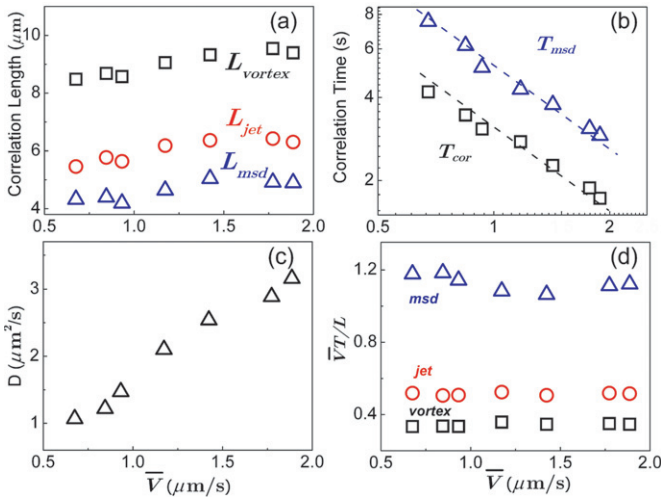

Fig. 5: (Color online) Correlation length L (a), correlation time T (b), diffusion constant (c) and a nondimensional number $(\overline{V}T)/L$ (d) as functions of mean speed $\overline{V}$. We note that a log-log frame is used in (b) and dashed lines have a slope of -1.

shown in fig. 4. The figure shows that both physical tracer particles (silica beads) and numerical tracers moving in the measured bacterial velocity field exhibit the same behavior: a short-time regime with nearly ballistic transport, $\langle \Delta r^2(\Delta t)\rangle \propto \Delta t^2$, and a longer-time regime where the transport is diffusive, $\langle \Delta r^2(\Delta t)\rangle \propto \Delta t$. The data are described by

$$\langle \Delta r^2(\Delta t)\rangle = 4D\Delta t \left(1 - e^{-\Delta t/T_{msd}}\right), \qquad (4)$$

where D is the diffusivity and the transition from the ballistic to the diffusive regime occurs at time T_{msd} and length scale $L_{msd} = \sqrt{\langle \Delta r^2(\Delta t = T_{msd})\rangle}$. For 1.3% agar concentration, we get $L_{msd} = 4.7\,\mu$m and $T_{msd} = 4.3$ s, scales comparable to those obtained from the velocity field data. This confirms the idea in [15] that the transition time and length scales in $\langle \Delta r^2(\Delta t)\rangle$ are determined by the time and length scales of coherent structures. The measured diffusivity, $D = 2.1\,\mu\text{m}^2/s$ for 1.3% agar concentration, is significantly larger than the thermal diffusivity for a micro-sphere with a diameter of 2 μm. Therefore, collective bacterial motion can transport and mix materials much more efficiently than thermal fluctuations.

To determine the relationship between the length, time, and velocity scales, we plot the extracted quantities (L_{vortex}, L_{jet}, and L_{msd}), time scales (T_{cor} and T_{msd}) and the diffusivity D as functions of mean speed $\overline{V}$ in fig. 5(a) to (c). The length scales are very weakly dependent on V_m, increasing by 10% from $\overline{V} = 0.7\,\mu$m/s (1.6% agar) to $\overline{V} = 1.9\,\mu$m/s (1.0% agar). The characteristic times are inversely proportional to mean speed. The measured diffusivity D is proportional to the mean speed (fig. 5(c)). Combining the information in figs. 5(a) and (b), we construct the nondimensional number $\overline{V}T/L$, which (within the experimental uncertainty) is independent of $\overline{V}$.

Discussion. – The constancy of $\overline{V}T/L$ (fig. 5(d)) indicates that the lifetime of the coherent vortices and jets is set by their size and the speed of the bacteria. While increasing the mean speed $\overline{V}$ has only a minor effect on the characteristic length scale (fig. 5(a)), the correlation time and diffusion depend strongly on $\overline{V}$ (figs. 5(b) and (c)). The behavior in figs. 5(a)–(c) is reminiscent of the "rate independence" for an individual swimmer in the Stokes flow regime[6] [28,29], but it is not clear how this rate-independence property can be preserved at colony level, where there are many factors beyond Stokes flow, including the free surface [30,31], stochastic run-and-tumble [8], and collisions between swimmers [10]. A model recently proposed by Wolgemuth [8] provides a plausible

[4]The movie `NumericalTracer.avi` shows trajectories of numerically integrated tracers plotted on phase-contrast images of bacteria. Data were obtained in a colony with 1.3% agar concentration. The image window is 115 μm × 115 μm. The movie is speeded up by 3 times.

[5]The movie `SilicaBeads.avi` shows motions of silica tracers with two typical trajectories overlayed. Data were obtained in a colony with 1.5% agar concentration. The image window is 115 μm × 115 μm. The movie is speeded up by 10 times.

[6]In Stokes flow regime, a bacterium swims through body deformation; the distance travelled by the bacterium between two different body configurations does not depend on the rate at which the deformation occurs.

explanation. In this model, the correlation length is determined by a competition between the local nematic alignment of rod-like bacteria and advection of the bacteria. The latter is set mainly by the propulsion force and a viscous drag coefficient. The strength of nematic alignment is assumed to be related to an energy scale estimated from translational diffusion and the drag coefficient. Assuming a bacterium generates the same propulsive force under different viscous conditions, we can simplify the scalings in [8] as follows: $L \propto \sqrt{\eta D}$ and $\overline{V} \propto \sqrt{D/\eta}$, where η is the dynamic viscosity of the fluid. Since $\overline{V} \propto D$ (fig. 5(c)), we have $\eta \propto 1/\overline{V}$; this yields L independent of $\overline{V}$, which is in reasonable accord with fig. 5(a).

The results in fig. 5(a) may also be consistent with the hypothesis of Copeland and Weibel [19]. They proposed that the high density of bacteria in swarming colonies and the large number of flagella per cell results in an intertwining of flagella of neighboring bacteria. This would lead to swarming with spatial correlations that depend weakly on the mean speed, which is in accord with our observations. This hypothesis could be checked by direct experimental observations in the future if a *P. dendritiformis* mutant with fluorescently labeled flagella becomes available.

In conclusion, our observations and analyses of the velocity field and tracer particle motion in swarming bacteria in *P. dendritiformis* colonies establish a relation between the mean speed of the bacteria and the characteristic length and time scales of the coherent vortices and jets that dominate the velocity field images (fig. 1): the coherent structures have lifetimes that are simply related to the size of the coherent structures and the average speed of the bacteria, $T \propto L/\overline{V}$. Further, the motion of tracer particles exhibits a crossover from short-time ballistic behavior to long-time diffusive behavior at a length scale that is approximately the same as the size of the coherent structures.

* * *

We thank E. Ben-Jacob and I. Brainis for providing the bacterial strain and the growth protocol. We are grateful to R. M. Harshey, I. S. Aranson, and C. Wolgemuth for fruitful discussions. We thank S. M. Payne for sharing incubator. ELF and HLS acknowledge support from the Robert A. Welch Foundation under grants F-1573 (ELF) and F-805 (HLS).

REFERENCES

[1] Narayan V., Ramaswamy S. and Menon N., *Science*, **317** (2007) 105; Aranson I. S., Snezhko A., Olafsen J. S. and Urbach J. S., *Science*, **320** (2008) 612; Narayan V., Ramaswamy S. and Menon N., *Science*, **320** (2008) 612.

[2] Kudrolli A., Lumay G., Volfson D. and Tsimring L. S., *Phys. Rev. Lett.*, **100** (2008) 058001.

[3] Ballerini M., Calbibbo N., Candeleir R., Cavagna A., Cisbani E., Giardina I., Lecomte V., Orlandi A., Parisi G., Procaccini A., Viale M. and Zdravkovic V., *Proc. Natl. Acad. Sci. U.S.A.*, **105** (2008) 1232.

[4] Makris N. C., Ratilal P., Symonds D. T., Jagannathan S., Lee S. and Nero R. W., *Science*, **311** (2006) 660.

[5] Vicsek T., Czirok A., Ben-Jacob E., Cohen I. and Shochet O., *Phys. Rev. Lett.*, **75** (1995) 1226.

[6] Sambelashvili N., Lau A. W. C. and Cai D., *Phys. Lett. A*, **360** (2007) 507.

[7] Toner J., Tu Y. H. and Ramaswamy S., *Ann. Phys. (N.Y.)*, **318** (2005) 170.

[8] Wolgemuth C. W., *Biophys. J.*, **95** (2008) 1564.

[9] Lega J. and Passot T., *Phys. Rev. E*, **67** (2003) 031906.

[10] Aranson I. S., Sokolov A., Kessler J. O. and Goldstein R. E., *Phys. Rev. E*, **75** (2007) 040901.

[11] Hernandez-Ortiz J. P., Stoltz C. G. and Graham M. D., *Phys. Rev. Lett.*, **95** (2005) 204501.

[12] Saintillan D. and Shelley M. J., *Phys. Rev. Lett.*, **99** (2007) 058102.

[13] Ishikawa T. and Pedley T. J., *Phys. Rev. Lett.*, **100** (2008) 088103.

[14] Dombrowski C., Cisneros L., Chatkaew S., Goldstein R. E. and Kessler J. O., *Phys. Rev. Lett.*, **93** (2004) 098103.

[15] Wu X. L. and Libchaber A., *Phys. Rev. Lett.*, **84** (2000) 3017.

[16] Sokolov A., Aranson I. S., Kessler J. O. and Goldstein R. E., *Phys. Rev. Lett.*, **98** (2007) 158102.

[17] Harshey R. M., *Annu. Rev. Microbiol.*, **57** (2003) 249.

[18] Verstraeten N., Braeken K., Debkumari B., Fauvart M., Fransaer J., Vermant J. and Michiels J., *Trends Microbiol.*, **16** (2008) 496.

[19] Copeland M. F. and Weibel D. B., *Soft Matter*, **5** (2009) 1174.

[20] Mendelson N. H., Bourque A., Wilkening K., Anderson K. R. and Watkins J. C., *J. Bacteriol.*, **181** (1999) 600.

[21] Steager E. B., Kim C. B. and Kim M. J., *Phys. Fluids*, **20** (2008) 073601.

[22] Be'er A., Smith R. S., Zhang H. P., Florin E. L., Payne S. M. and Swinney H. L., *J. Bacteriol.*, **191** (2009) 5758.

[23] Be'er A., Zhang H. P., Florin E. L., Payne S. M., Ben-Jacob E. and Swinney H. L., *Proc. Natl. Acad. Sci. U.S.A.*, **106** (2009) 428.

[24] Ben-Jacob E., Cohen I. and Levine H., *Adv. Phys.*, **49** (2000) 395.

[25] Harshey R. M., private communication (2009).

[26] Hernandez-Ortiz J. P., Underhill P. T. and Graham M. D., *J. Phys.: Condens. Matter*, **21** (2009) 204107.

[27] Debenedetti P. G. and Stillinger F. H., *Nature*, **410** (2001) 259.

[28] Purcell E. M., *Am. J. Phys.*, **45** (1977) 3.

[29] Lauga E. and Powers T. R., *Rep. Prog. Phys.*, **72** (2009) 096601.

[30] Baskaran A. and Marchetti M. C., *Phys. Rev. Lett.*, **101** (2008) 268101.

[31] Trouilloud R., Yu T. S., Hosoi A. E. and Lauga E., *Phys. Rev. Lett.*, **101** (2008) 048102.